Macromolecules

ARTICLE

pubs.acs.org/Macromolecules

Importance of Covalent Linkages in the Preparation of Effective Reduced Graphene Oxide–Poly(vinyl chloride) Nanocomposites

Horacio J. Salavagione* and Gerardo Martínez

Instituto de Ciencia y Tecnología de Polímeros, CSIC, Juan de la Cierva 3, 28006 Madrid, Spain

Supporting Information

ABSTRACT: The preparation of nanocomposites of reduced graphene oxide (RGO) with poly(vinyl chloride) (PVC) is reported. Covalent modification of PVC with RGO and reduction/precipitation of graphite oxide and isocyanates-modified GO in the presence of PVC are studied. Among these methods it is proposed that only the former produces nanocomposites with enhanced final properties. The other method failed because it did not produce nanocomposites with different properties to the original polymer, probably due to the lack of effective interfacial interactions. The RGO-chemically modified PVC samples have different thermal and mechanical properties with respect to the parent polymer. A discussion on the dependence of the properties on the method of preparation is given. Furthermore, preliminary results based on the effect of the aspect ratio and surface chemistry of the filler are also given.

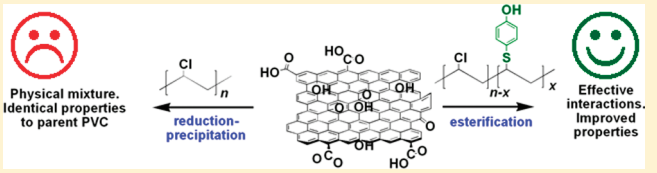

INTRODUCTION

In recent years graphene, consisting of one- or several-atom-thick two-dimensional (2D) graphite layers, has attracted considerable attention.[1,2] In fact the rapid growth in the study of its synthesis, properties and the development of applications has led its discoverers to receive the Nobel Prize in Physics 2010. Compared to carbon nanotubes (CNTs), as well as high aspect ratio and low density, graphene is being deeply investigated because of its unique and outstanding mechanical, electrical and electronic properties that result in it being one of the most popular candidates for the development of functional and structural graphene-reinforced composites.[3−11] Indeed, graphene-based polymer nanocomposites[2] is a rapidly growing area of nanoengineered materials, providing lighter weight alternatives to CNTs-based nanocomposites with additional functionality associated with nanoscale specific, value-added properties. As occurred with other nanofillers, such as CNTs, montmorillonite, etc., the maximum improvements in final properties can only be achieved when graphene is homogeneously dispersed in the matrix and the external load is efficiently transferred through strong filler/polymer interfacial interactions.[12,13] Thus, the design of the method of preparation may be essential to generate graphene-based nanocomposites with effective polymer/graphene interactions.

Graphene reinforcement has already been used in almost all types of polymers comprising olefin,[14] acrilic,[3] styrene,[4] and vinyl,[8] as well as conducting polymers.[15,16] With regard to the preparative methods, graphene has been effectively dispersed in polymers having aromatic groups in the main chain, e.g., poly(styrene) (PS) by different methodologies including mixing PS with appropriately modified graphite oxide (GO) followed by reduction and precipitation[4] as well as using a GO derivative as initiator of polymerization.[17] In vinyl polymers, Ansari and Giannelis reported a comparative study of poly(vinylidene fluoride) nanocomposites based on functionalized graphene sheets and exfoliate graphite.[18] The composites, prepared using solution processing followed by compression molding, were characterized in terms of their electrical, mechanical, and thermal properties. Moreover, nanocomposites of graphene with poly(vinyl alcohol) (PVA) have been extensively studied[5,8,19,20] and the incorporation of graphene has been approached by reduction of GO and precipitation in the presence of the polymer[8] as well as by direct esterification among the carboxylic groups in GO and the hydroxyl groups in PVA.[21] The differences in the final properties were strongly dependent on the procedure employed. However, although the esterification approach appears to be the best to ensure good graphene dispersion, it has not been widely exploited as yet.

On the other hand the important position held by poly(vinyl chloride) (PVC) in the commercial polymer market has meant inevitably that a considerable amount of research has been devoted to various aspects of its preparation, processing, and properties. PVC is a well-known atactic polymer with a stereochemical composition that can be manipulated over a narrow range by performing the polymerization at different temperatures. The preparation of graphene/PVC nanocomposites has been recently addressed from sonicated graphite flakes.[22] Although effective interactions between pure graphene and PVC seem to be difficult to visualize due to the lack of functional groups in graphene, the authors reported improvements in the mechanical, thermal and electrical properties. However they did not elaborate any discussion on the nature of such interactions.

Received: December 23, 2010
Revised: March 15, 2011
Published: March 28, 2011

More attractive, GO has oxygenated groups that can, in principle, interact with the chlorine atoms in PVC by halogen bonding[23,24] or can serve as active sites to anchor functional groups to make GO compatible with PVC, e.g., by inducing solubility in solvents in which PVC is soluble. Indeed, Ruoff and colleagues have reported the functionalization of GO with a series of organic isocyanates producing materials soluble in *N*,*N*-dimethylformamide (DMF),[25] a good solvent for PVC. Therefore, to explore these possibilities and prepare useful nanocomposites a detailed study on the methods of preparation and consequently the potential filler/polymer interactions should be undertaken. However, we should previously answer some important questions: First, can GO interact with PVC by halogen bonding? Second, in the case that it occurs, is this halogen bonding strong enough to ensure changes in the final properties? And finally, is further modification of GO required to ensure these interactions?

Recently we have demonstrated that PVC can be covalently functionalizated with CNTs from a stereoselective nucleophilic substitution reaction that allow us to merge the control of the reaction and the good properties of CNTs and, consequently, to enhance the properties of the PVC.[26] We observed that the molecular level coupling between CNTs and the polymer chain not only change the mobility and enhance the stability of the PVC chain but also it supported our opinion that molecular level couplings determine the mechanical properties of CNT based composites. In principle, this procedure can be extended to covalently modify PVC with graphene.

In this paper we describe a series of experiments carried out to incorporate graphene into PVC and to obtain nanocomposites with improved properties. We used the reduction of GO and isocyanate-modified GO (*i*-GO) in the presence of PVC as well as the covalent incorporation of graphene by esterification of GO with appropriately modified PVC. We intend to demonstrate that the final properties of the materials strongly depend on the method of preparation. While the first methodology produces composites that resemble a physical mixture with properties very close to that of the parent PVC, the covalent modification significantly alters the properties of the matrix. We concluded that, in this particular case that covalent attachment is the only tool that allows us to prepare a nanocomposite with efficient filler/polymer interactions leading to nanocomposites with improved properties.

EXPERIMENTAL SECTION

Materials. A PVC sample was prepared at 90 °C in a bulk polymerization process (20% conversion) with 2, 2′-azobis(isobutyronitrile) (AIBN) as an initiator. The degree of isotacticity was determined by FTIR and ^{13}CNMR. The graphite used in this study was natural flake graphite (Aldrich) which has an average diameter of 45 μm. Tetrahydrofuran, THF (Ferosa), cyclohexanone, CH (Aldrich), dimethylformamide, DMF (Aldrich), and hexamethylphosphoric triamine, HMPT (Aldrich), were purified by fractional distillation under nitrogen immediately before being used. Phenyl isocyanate, *N*,*N*-dicyclohexylcarbodiimide (DCC), 4-dimethylaminopyrydine (DMAP, 99%), 4-hydroxythiophenol (HT), hydrazine, and sodium borohydride ($NaBH_4$) were purchased from Aldrich and used as received. Equimolecular amounts of HT and potassium carbonate (K_2CO_3) were used to form 4-hydroxythiophenolate anion *in situ* in CH.

Procedure I. Reduction in the Presence of the Polymer. *Preparation of RGO/PVC Samples.* GO was prepared according to the Hummers method.[27] A 400 mg sample of graphite powder, 200 mg of sodium nitrate and ∼10 mL of concentrated H_2SO_4 were mixed and cooled to 0 °C, and the solution was maintained under vigorous stirring. Next, 1.2 g of $KMnO_4$ was added to the solution in stepwise manner so that the temperature was kept <20 °C during the $KMnO_4$ addition steps. After the complete addition of $KMnO_4$ the temperature of the solution was slowly raised to 35 °C and maintained for 30 min. A brownish-gray paste was formed. Next, ∼40 mL of deionized water was added to the solution, which turned brownish-yellow. Subsequently, the temperature of the solution was increased to 98 °C during the addition of water and this temperature was maintained for 15 min. The solution was then mixed with 56 mL of warm water followed by addition of 4 mL of 3% H_2O_2 that reduces the residual permanganate. The light yellow particles were washed thoroughly with warm water 7−8 times. After the resulting mixture was filtered, the precipitate was washed with 10 wt % of aqueous HCl solution to remove remaining metal ions, followed by further washing with deionized water several times, and finally dried at 60 °C under vacuum.

A PVC/GO nanocomposite with 5 wt % of filler was prepared as follows (Scheme 1): 0.05 g of GO was dissolved in 20 mL of DMF and treated with ultrasound for 2 h. Subsequently, 0.95 g of PVC was poured into the GO solution. The mixture was maintained under magnetic agitation for 4 h. The subsequent reduction of GO was accomplished by adding 0.4 g of $NaBH_4$ to the PVC/GO solution with magnetic stirring at room temperature for 20 h. After this time the initial brownish reaction media became black, indicating the reduction of GO to reduced graphene oxide (RGO). The polymer nanocomposites were coagulated with methanol under vigorous stirring. The gray solid nanocomposites were filtered, washed abundantly with methanol and dried under vacuum for 24 h. The reduction was confirmed by FTIR where the signals corresponding to oxygenated groups disappeared or diminished in intensity (Supporting Information, Figure S1).

Preparation of i-RGO/PVC samples. GO was reacted with phenyl isocyanate according to ref 25 (Scheme 1). Briefly, 0.5 g of GO was dissolved in 50 mL of anhydrous DMF, and then 2.5 mL of phenyl isocyanate was added. The mixture was allowed to react at room temperature for 24 h. The product was precipitated with methylene chloride. The final i-GO was filtered, washed with additional methylene chloride and dried under vacuum.

i-RGO nanocomposites with 1, 1.5, 2, 3, 5, and 10 wt % of filler (Table 1) were prepared following the procedure described for GO/PVC giving a dark gray solid. The FTIR spectrum shows new bands corresponding to the isocyanate group. The reduction was also confirmed by FTIR as in the case of RGO-PVC.

Procedure II. Grafting GO on Modified PVC. PVC was modified with potassium 4-hydroxythiophenolate (KHT) by a nucleophilic substitution reaction according to ref 26. The final product was named mPVC. The esterification procedure employed for GO was as follows (Scheme 1): 40 mg of GO and 0.4 g of mPVC were suspended in CH (20 mL). The suspension was gently stirred and maintained at 70 °C under nitrogen for 72 h. Then, a solution of DCC (1.84 g, 9 mmol) and DMAP (0.136 g, 1.1 mmol) in CH (20 mL) was added, and the resulting mixture was stirred at 40 °C for another 72 h. Coagulation of the polymer nanocomposite was accomplished by adding the suspension into a large excess of methanol under vigorous stirring. The solid nanocomposite (named GO-e-PVC) was filtered, washed with methanol and dried at 50 °C under vacuum. In order to remove the rest of nonreacted GO, the solid was redissolved in THF, centrifuged at a high speed (16 000 rpm) for 30 min and the supernatant solution coagulated with methanol. The procedure was repeated twice and 388 mg of a gray solid (yield = 97%) was obtained after vacuum-drying at 50 °C for 30 h. Generally, the reduced graphene oxide−PVC (RGO-e-PVC) was prepared by vigorously stirring a solution of 170 mg of GO-e-PVC and 1.5 mL hydrazine hydrate in 30 mL of CH at 90 °C for 5 h. The solution

Scheme 1. Diagram Representing the Explored Strategies to Prepare PVC/RGO Composites

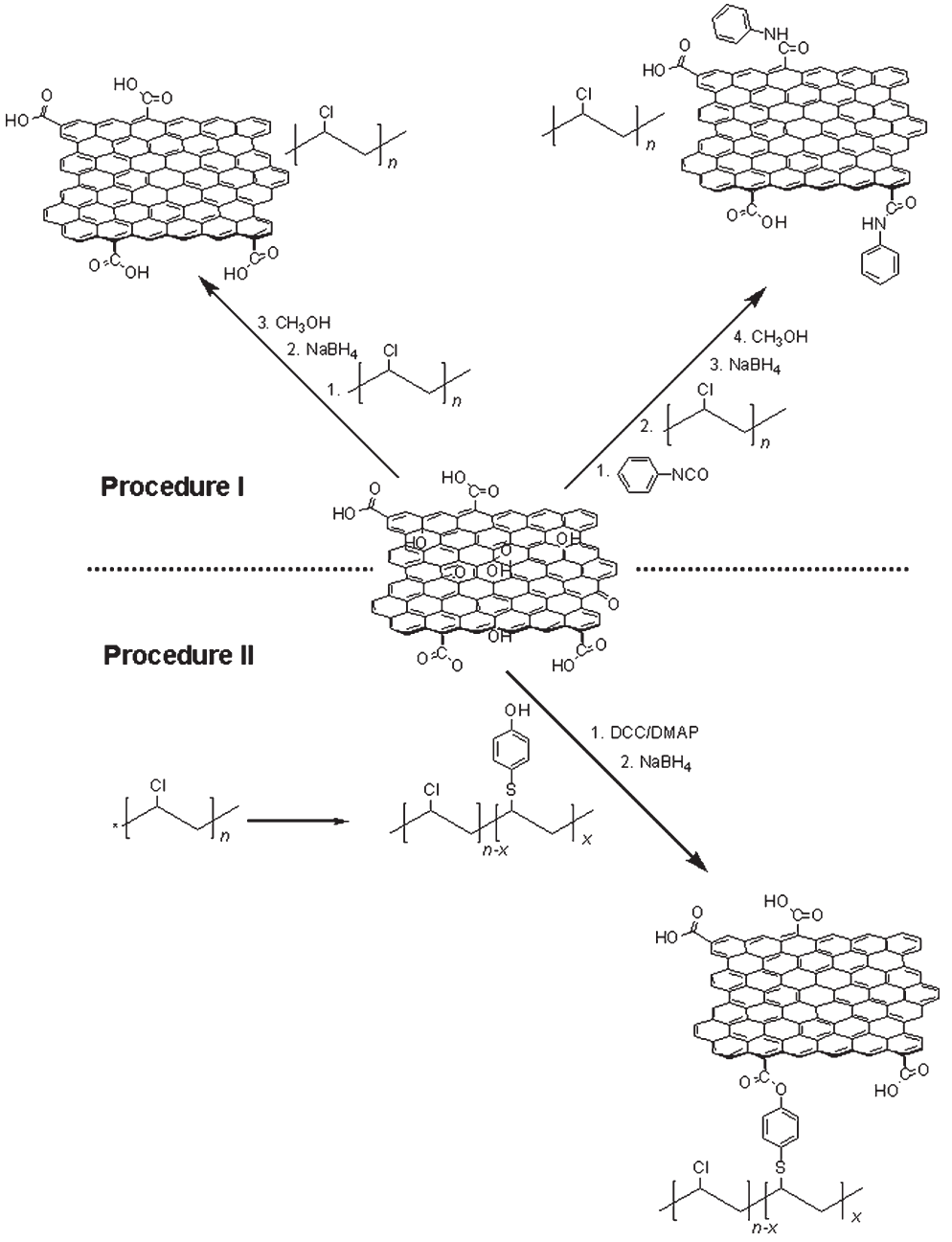

was kept at room temperature overnight to ensure complete reduction. Subsequently, the RGO-e-PVC was collected and purified by washing with methanol and water several times to remove any free hydrazine. The product was soluble in common organic solvents such as THF, CH, dioxane, and DMF, similar to the parent PVC.

It should be pointed out that although we have used a different reducing agent than in the previous procedure, the agents were choosing as a function of the reaction media. Notwithstanding, the experimental conditions in both cases ensure complete reduction of basal plane of GO to RGO.

Characterization. The density of parent PVC and RGO-e-PVC nanocomposites was measured at 25 ± 0.1 °C with a capillary pycnometer (50 mL). The immersion liquid was methanol. Films were prepared via casting from THF solutions (100 mg mL^{-1}) on glass plates and then extracted with diethyl ether in a Soxhlet for 3 days. Only the samples of ~0.15 g that did not contain visible bubbles or pores were examined. The error in the measurements was estimated to be less than ±0.2%.

The FTIR measurements were carried out on a Perkin-Elmer System 2000 FTIR spectrometer equipped with a deuterated triglycine sulfate detector (DTGS) using a resolution of 2 cm^{-1}. The powdered samples were thoroughly mixed with KBr and pressed into pellet form. Because of the hydroscopic behavior of KBr, the sample cell was purged with desiccated air.

^{1}H NMR spectra were recorded at 400 MHz on a Varian Inova 400 spectrometer with dioxane-d_8 as the solvent and locking agent at 80 °C under standard conditions. The tacticity of parent PVC, the mPVCs, and the GO-e-PVC samples were measured by means of ^{13}C NMR decoupled spectra obtained at 80 °C using a Varian Unity instrument operating at

dx.doi.org/10.1021/ma102932c |*Macromolecules* 2011, 44, 2685–2692

Table 1. Composition, T_g, and Decomposition Rate Values of All Samples Used in This Study

method	sample	RGO content/wt %	T_g/°C	decomposition rate/$\times 10^2$% min^{-1}
	PVC		81.8	1.6
procedure I	i-RGO/PVC01	1	84.5	5.2
	i-RGO/PVC02	1.5	81.6	5.6
	i-RGO/PVC03	2	80.6	8.3
	i-RGO/PVC04	3	83.2	11
	i-RGO/PVC05	5	84.9	18
	i-RGO/PVC06	10	82.9	22
	RGO/PVC	5	84.7	---
procedure II	RGO-e-PVC1	1.2[a]	102	---
	RGO-e-PVC2	1.4[a]	106.7	1.2

[a] Calculated by ^{1}H NMR.

125 MHz in dioxane-d_8 solutions. The spectral width was 2500 MHz and a pulse repetition rate of 3 s and 16,000 data points were used. The relative peak intensities of the spectra were measured from the integrated peak areas, calculated by means of an electronic integrator.

The dispersion of the nanofiller was examined using a Philips XL30 ESEM equipment. The nanocomposite samples were cryofractured from film specimens, prepared as detailed below, and then were covered with ca. 5 nm Au/Pd overlayer to avoid charging during electron irradiation.

To obtain the glass transition temperatures (T_g), differential scanning calorimetric (DSC) thermograms were conducted on 8−10 mg samples at a heating rate of 10 °C/min with a Mettler TA4000/DSC-30 system calibrated with an indium standard. Dry nitrogen was used as the purge gas. The samples were scanned twice, and the T_g was taken as the midpoint between the intersections from the glassy state to the liquid state of the second scan. The reproducibility of duplicate runs of samples with well-defined T_g's was better than ±0.2 °C.

The thermograms of the individual polymers and the nanocomposite powder samples were performed with a Mettler TA4000/TG50 thermogravimetric analyzer (TGA) on 5−10 mg samples. The weight percentage of remaining material in the pan was recorded during heating from 50 to 700 °C at a heating rate of 10 °C/min. Nitrogen was used as the purge gas. Isothermal experiments were carried out at 160 °C for 1 h. UV−visible absorption spectra of degraded samples in HMPT solutions (of ca. 0.5 mg mL^{-1}) were measured using a Perkin-Elmer UV−vis Lambda 16 spectrometer at room temperature.

The dynamic mechanical performance of the polymers was studied using a Mettler DMA 861 dynamic mechanical analyzer. For DMA measurements film samples were prepared by casting and evaporation from a 100 mg mL^{-1} solution of the modified polymer in THF and then cut into specimens of 4 mm ×19 mm and ∼0.1 mm thick. After mounting the sample in the tensile mode, the furnace was sealed off, scanned over a temperature range from −100 to +110 °C at fixed frequency of 1 Hz. The heating ramp rate was 2 °C/min. A dynamic force of 6 N was used oscillating at fixed frequency and amplitude of 30 μm. The tan δ (ratio of the loss to storage modulus) has been determined during the test as a function of increasing temperature.

RESULTS AND DISCUSSIONS

It is widely known that in graphene-based nanocomposites, control of the size, shape, and surface chemistry of the reinforcement materials are essential in the development of materials that can be used to produce devices, sensors and actuators based on the manipulation of functional properties. In this work the samples obtained by the two procedures were characterized by SEM in order to determine the presence of graphene dispersed in the matrix and FTIR to give a preliminary examination on the existence of some kind of interactions. However, the best method to examine effective filler/polymer interactions is the direct measurement of the final thermal, mechanical and/or electrical properties.

First we investigated the success of the esterification of PVC with GO (procedure II). The FTIR spectrum of the GO-e-PVC shows absorption bands characteristic of the mPVC (signals at 1497, 1587, and 1602 cm^{-1} corresponding to the aromatic C═C vibration modes, and a band around 3400 cm^{-1} due to hydroxyl function) overlapped with new bands (Figure1a). The effective linkage between the GO and the mPVC is evident from FTIR spectrum, which shows a band at 1658 and 1737 cm^{-1} corresponding to C═O stretching of carboxylic acid and ester groups, respectively. The ^{1}H NMR spectrum of the GO-e-PVC in deuterated dioxane is quite different from that of the corresponding mPVC, especially in the zone of the aromatic (7.5−6.9 ppm) and hydroxyl protons (7.9 ppm) (Figure 1b). First, the intensity of the hydroxyl proton peak remarkably decreases after the esterification reaction. On the other hand, two new signals at 7.21 and 7.62 ppm appear. These signals correspond to aromatic protons in a different environment and can be due to the influence of the carbonyl of the ester group on the protons of the benzene ring.[26] As was explained for CNTs-modified PVC, the discrimination of both types of protons, i.e. protons of the GO-mPVC samples and protons of the mPVC units, allows us to evaluate the percentage of GO in the sample.[26] On the basis of the integration of the signals the amount of GO in GO-mPVC was estimated to be about 1−2 wt % units based on total composition.

The FTIR spectra of the nanocomposites prepared by all methods are quite similar, except in the region between 600 and 700 cm^{-1} (ν C−Cl vibrations) where some slight differences can be observed (Figure 1c). While no changes have been observed for the samples GO/PVC and i-GO/PVC, some differences in the GO-e-PVC sample have been detected. The frequencies at 615 and 637 cm^{-1} remain unaltered in the unmodified regions of the PVC. The bands at 615 and 637 cm^{-1} obey S_{HH} absorption modes of the C−Cl bond (the suffix stands for the trans susbtituents on both C−C bonds adjacent to the C−Cl bond) and are very sensitive to the local chain conformations and, owing to the microstructure dependence of the latter, to the local microstructure of the polymer. Further, each of these frequencies has been shown to depend on the local environment.[28] Figure 1c shows the 500−700 cm^{-1} region of the FTIR spectrum of the virgin PVC sample and the same sample after covalent incorporation of GO. The following changes in the grafted samples can be explained: (i) the intensity of the band at 615 cm^{-1}

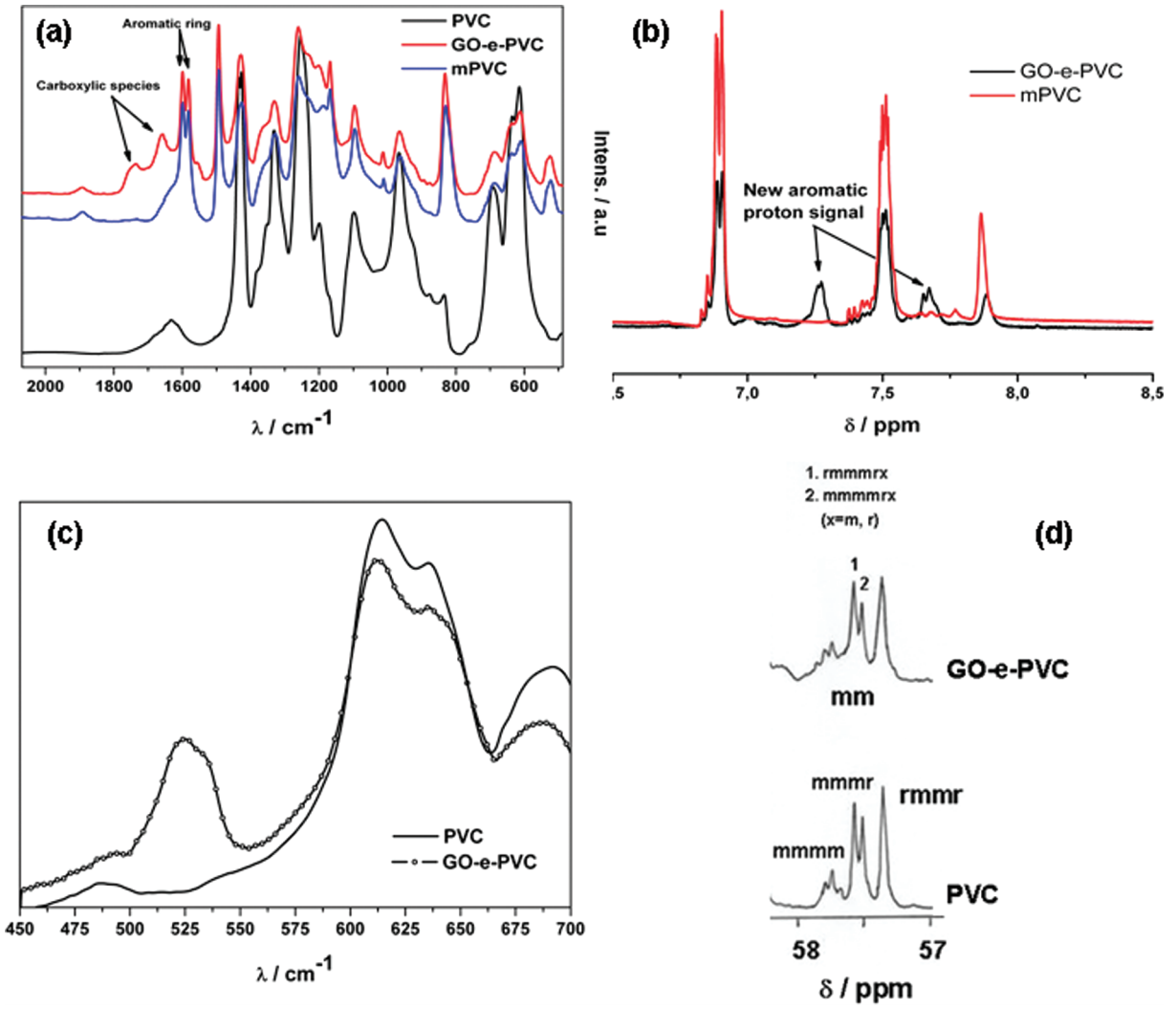

Figure 1. Spectroscopic characterization of PVC esterified with GO. FTIR (a) with enlarged view highlighting the area of C−Cl vibration (c), ^{1}H NMR in deuterated dioxane and (b) and ^{13}C NMR in the region containing information about the tacticity (d).

increases compared to that of the 637 cm^{-1} band. The band at 637 cm^{-1} seems to decrease in a parallel manner, although to a lesser extent, to the increase of the 615 cm^{-1} band, and (ii) there is some broadening of the absorption around 637 cm^{-1}. It is worth emphasizing that the increase of $A_{615\ cm^{-1}}/A_{637\ cm^{-1}}$ band ratio is similarly observed in the substitution reaction of PVC with 4-hydroxythiophenolate and the broadening around 637 cm^{-1} is consistent with the appearance of S_{HH} structures of C−Cl bonds in all-trans syndiotactic triad conformations as a result of the stereospecific mechanism in modified PVC[26] and consequently in the polymer-grafted GO.

Once the covalent incorporation of GO to mPVC was demonstrated, special interest has been paid to confirm that the substitution reaction proceeds through a stereoselective mechanism thus leading to a stereoselective incorporation of GO. In a similar way to the preceding work with CNTs,[26] we have studied the evolution of PVC tacticity in both the modified polymer and the corresponding GO-e-PVC by high resolution ^{13}C NMR spectroscopy. Figure 1d shows the ^{13}C NMR spectra (methynic region of isotactic triads) of the samples. It can be seen that the resolution of the spectra allows an accurate determination of the content of the pentads centered around one isotactic triad. From the integration of the content of the *mmmr* pentad (57.6−57.4 ppm), the changes in *rmmmrx* (*x* = *m* or *r*) heptads, may be calculated at least to some extent. It appears evident that the overall decrease of *mmmr* content is chiefly related to the specific disappearance of the heptad *mmmmrx* (*x* = *m* or *r*). It is observed that the decrease of the 57.50 ppm signal corresponding to *mmmmrx* (*x* = *m* or *r*) is more pronounced than that at 57.56 ppm for *rmmmrx* (*x* = *m* or *r*). Thus, the reactivity of *mmr* proves to be much more accentuated as the length of the associated isotactic sequence increases. Consequently, the increase of the *rmmmrx*/*mmmmrx* ratio (1.32 for GO-e-PVC1 vs 1.14 for parent PVC) definitely confirms the stereoselective nature of the attachment of GO to the PVC.

The aforementioned results suggest that there are no interactions among GO and i-GO with PVC or that the interactions are so weak to be detected by inspection of the C−Cl FTIR bands. For instance, nanocomposites of RGO/PVA prepared by reduction/precipitation revealed interactions between the GO and the matrix probably by hydrogen bonding.[8] Clearly hydrogen bonding is stronger than halogen bonding and more likely to produce changes in the vibrational spectrum.

Regarding the morphology of the samples, no differences between the samples obtained by both procedures were observed

(Figure S2, Supporting Information), limiting the study to only one parameter: the surface chemistry that governs the interfacial interactions.

In order to prove this hypothesis, the thermal parameters, stability and electrical conductivity were investigated by DSC, TGA, and four-probe conductivity measurements, respectively. Substantial differences in the thermal behavior were observed, but in both cases the final products were electrically nonconducting. The lack of conductivity has a different explanation depending on the preparative method employed. For composites prepared by procedure I, the composites remain nonconductive even at high RGO contents (10 wt %). Clearly to surpass the percolation limit the RGO should be well dispersed in the PVC matrix and this dispersion strongly depends on interfacial filler/polymer interactions. It seems that in this case no effective interfacial interactions take place, as will be demonstrated below. In the case of grafting RGO to PVC, the strong steric effect by introducing huge graphitic laminates controls the degree of functionalization. Therefore, in spite of the high aspect ratio of RGO, it is possible that its concentration remains below the percolation threshold

With regard to the DSC results, parent PVC has a T_g at 81.8 °C. For the samples prepared by reduction/precipitation this value remains unaltered and shows no dependence on the graphene content, suggesting that no actual interaction GO/PVC or i-GO/PVC occurs (Table 1). Therefore, the segmental mobility of PVC chains is essentially the same in both the absence and presence of graphene, which means that these samples behave as physical mixtures. However, the GO-e-PVC samples show a significantly different behavior with the value of T_g shifted by around 30 °C (Table 1). Although variations in T_g are also observed after the modification of PVC by nucleophilic substitution, it is evident that graphene influence the mobility of the polymer chains conferring rigidity to the system. The displacement of the value of T_g for GO-e-PVC is even larger than that observed for the esterification of the same PVC with CNTs.[26] A detailed discussion comparing the results from both types of samples will be given later.

The thermal stability of the nanocomposites is also influenced by the preparative methods and consequently depends on the interfacial interaction. However the explanation for the results encountered is somewhat more complex. Dynamic TGA curves of all samples prepared by reduction/precipitation are identical to those of pure PVC (Supporting Information, Figure S3) confirming that the system behaves like a physical mixture since the PVC degrades as in the absence of graphene. However, the curve for GO-e-PVC shows an onset of degradation at lower temperatures (Supporting Information, Figure S4). This effect corresponds to the decrease in stability caused by the preliminary nucleophilic substitution of PVC with HT required to make PVC suitable for esterification. In fact, the PVC decomposition occurs at 290 °C whereas for the mPVC it takes place at 265 °C. This decrease has been assigned to a change in the global process of degradation. Since it has been reported that the nucleophilic substitution of PVC proceeds through a stereoselective mechanism,[26,29,30] it was proposed that a selective substitution brings about a strong progressive stabilization until a degree of substitution of ~1% is attained. Afterward, the stability decreases with increasing degree of substitution. These effects were proposed to result respectively from the lability of some chlorine atoms located at *gttg*$^-$ and *tttg* conformations that disappear by selective substitution and from the favored buildup of all-trans polyenes upon initiation at syndiotactic sequences.[31]

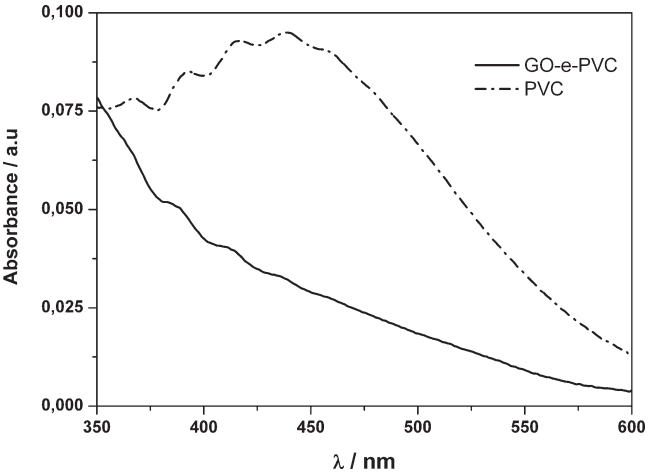

Figure 2. UV−visible spectra after isothermal treatment at 160 °C for 1 h of (a) pristine PVC and (b) GO-e-PVC.

It is evident that in dynamic TGA experiments it is difficult to obtain a visual display of initial steps of thermal degradation. In order to elucidate this point we analyzed the degradation at low conversion, where the influence of chain conformations in the degradation process is more apparent. With this objective isothermal degradation was undertaken for all samples at 160 °C for 1 h in a nitrogen atmosphere, which represents ~1−2% weight loss. While the results obtained for GO-e-PVC were similar to that for CNTs-covalently modified PVC[26] demonstrating higher stability, the isothermal degradation for iGO/PVC nanocomposites showed a higher degradation rate. The results obtained from the isothermal degradation of GO-e-PVC clearly demonstrate higher stability, in fact the parent PVC has a degradation rate of 1.6×10^{-2}% min^{-1} compared to 1.2×10^{-2}% min^{-1} observed for the GO-e-PVC sample, which represents a degree of stabilization of around 25% (Table 1).

It is well established that the thermal degradation of PVC leads to the formation of polyene sequences as a result of the sequential elimination of hydrogen chloride. The characterization of these polyene sequences has been undertaken by UV/visible spectroscopy by assuming that the observed spectrum is the resultant of the overlapping spectra of a range of polyenes with different conjugated sequence lengths.[31] Consequently, the thermal stabilization of GO-e-PVC should be strongly related with a strong reduction in the content of long polyene sequences compared with the parent PVC. This is in fact observed when we compare the UV−vis spectra of both samples after isothermal degradation at 160 °C (Figure 2).

On the other hand, the degradation rate of i-GO/PVC at low conversion increases as the RGO content increases (Table 1). Although based on the above results we proposed that the sample behaves as a physical mixture, it seems that the graphitic materials catalyze the degradation at the earlier step by providing active sites to initialize the degradation of PVC.

The most important conclusion from the above results is that the covalent attachment of graphene to the PVC emerges as the only effective route to produce a new material with enhanced properties with respect to the parent PVC. Once this has been assumed, we will highlight some features of the influence of the aspect ratio and surface chemistry of graphitic material on the final properties of nanocomposites.

In order to investigate whether the higher aspect ratio of graphene has more influence on the final properties of PVC than CNTs, we compared the thermal and mechanical properties of

Scheme 2. Diagram Representing the Changes in the Sample Volume with Reduced Mobility on the Basis of the Formation of Secondary Bonds between Oxygenated Groups in GO and RGO with Moieties in Modified PVC

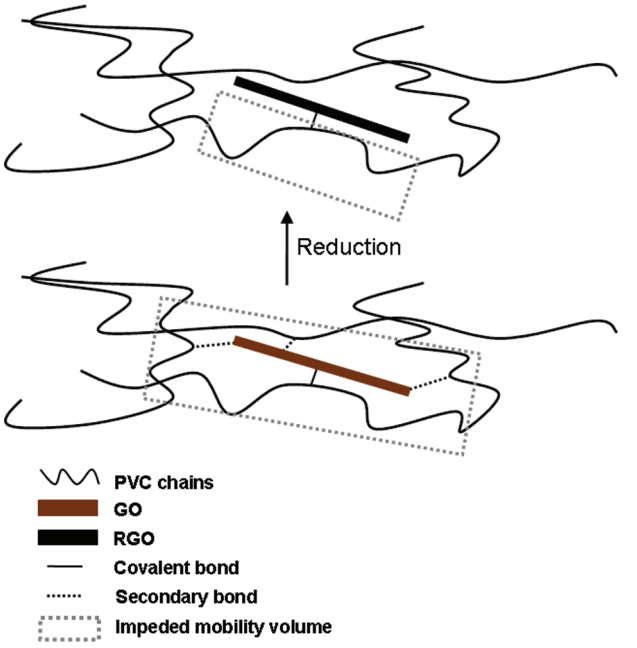

RGO-e-PVC and CNTs-e-PVC with the same degree of modification of PVC and similar composition of carbonaceous materials (~1.3 wt % for MWNTs and 1.2 wt % for GO and RGO). As mentioned earlier, the T_g is almost two degrees higher for RGO-e-PVC than that for CNTs-e-PVC that may be an indication of a slight influence of the higher aspect ratio of RGO. In this context, it is important emphasize in the case of the samples RGO-e-PVC that at higher degrees of modification of PVC, and consequently slightly higher degree of incorporation of graphene in the polymer, the values of T_g are always higher that those of the modified polymer (Supporting Information, Figure S5). This result suggests the existence of a dual phenomenon. On the one hand the evolution of T_g in GO-e-PVC with respect to the CNTs-e-PVC in comparison with the modified polymer as a result of the stereoselective character of the grafting reaction, and the local conformational rearrangements in the preliminary modification reaction of the PVC, indicate that GO platelets must in some way occupy space of the large free-volume ascribed to the $gttg^{-}tt$ conformation connected with sufficiently long sequences, increasing packing density. This was confirmed comparing the values of density between the parent PVC (1.38 g/cm^3) with that of the RGO-e-PVC nanocomposite sample (1.42 g/cm^3) that is in accordance with a preceding result for PVC graft copolymers.[30] On the other hand, the incorporation of graphene in the polymer not only restricts the mobility of the polymeric chain in the zones of higher free volume, that correspond to the zones of higher isotactic content as in the case of CNT, but such mobility remains also restricted to a higher degree of modification and therefore of graphene in heterotactic segments. This result only can be explained by admitting strong interactions between the plates of GO and RGO and the adjacent polymer segments, especially the former (Scheme 2).

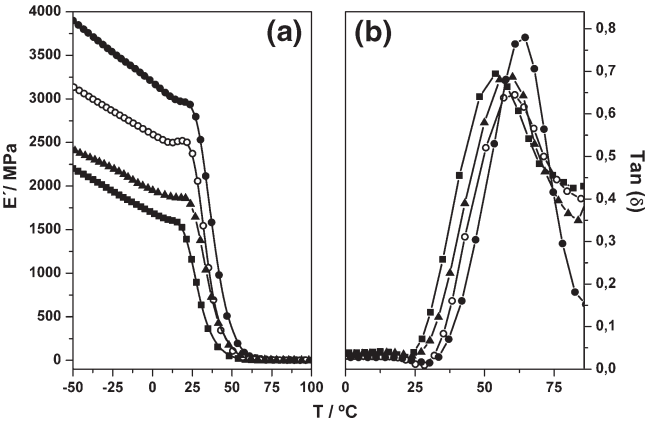

Figure 3. Comparison of (a) storage modulus and (b) tan δ curves for mPVC (square), CNTs-e-PVC (triangle), GO-e-PVC (solid circle), and RGO-e-PVC (open circle).

Also, more pronounced changes were observed for the storage modulus (E') as a function of temperature (Figure 3). The samples were referred to the starting modified PVC for clarity. The modulus at 1 Hz and room temperature are 1100 MPa for mPVC, 1830 MPa for CNTs-e-PVC, and 2326 MPa for RGO-e-PVC and 2960 MPa for GO-e-PVC. Therefore, RGO shows improved reinforcement compared to CNTs, probably due to higher interfacial interactions derived from the higher aspect ratio. Furthermore, the shift of T_g with respect to the parent PVC obtained by DMTA experiments is similar to that observed by DSC.

Finally, we will discuss the effect of the surface chemistry of the filler on the mechanical properties of the polymer. Comparing the DMTA results of PVC esterified with GO before and after reduction, the reduced material shows poorer properties since it has a ~20−25% lower storage modulus. This observation suggests that the interfacial contact is more intimate in the case of the unreduced filler. Since the degree of covalently bonded graphitic material in both cases is the same, the only differences lie in the oxygenated groups in the GO that can form some secondary intra or interchain bonding with the mPVC. Considering the structures of both components, the secondary bonds may be as follows: (i) halogen bonding between oxygenated groups in GO or RGO and chlorine in PVC, (ii) $\pi-\pi$ among graphitic materials and the benzene ring of the nucleophile, and (iii) hydrogen bonding of hydroxyl groups of the nucleophile with oxygenated groups in GO. The first can be discarded because the nanocomposites prepared by reduction/precipitation did not show any changes with respect to PVC as demonstrated above. The $\pi-\pi$ interactions are not responsible because this would be stronger in the case of RGO. Therefore, the third option emerges as the secondary bond responsible for the changes in the mechanical properties as the probability of forming hydrogen bonding is higher in GO than in RGO, which only retains carboxylic groups at the edges. Therefore, *a priori*, it seems that the RGO stiffens only one segment of specific length in the chain to which it is attached, while the GO also alters the stiffness of adjacent chains or more segments of the same chain (Scheme 2). In addition, the existence of this type of secondary bonds will increase the density of filler/polymer interactions thus improving the filler dispersion into the polymer matrix.

Though it is well-known that the incorporation of nanoparticles into a polymer host induces significant changes in the dynamical behavior of the polymer, the present results reveal the role that conformational changes and cooperative effects, i.e., interactions, can have on the mobility and, consequently, on the final properties of materials with covalent attachment of graphene to PVC. This emphasizes the importance of deeper studies of the effects of confinement on the local dynamics of graphene-based polymer nanocomposites. In this context, new strategies and experiments, including the chemical modification of the GO with appropriate moieties to compatibilise it with PVC are currently underway.

CONCLUSIONS

Several methodologies to prepare RGO/PVC nanocomposites and the optimum conditions have been established. The covalent attachment of RGO to appropriately modified PVC is the only effective method to produce nanocomposites with improved thermal and mechanical properties. The absolute values of the mechanical and thermal properties of RGO-e-PVC are higher that those for a similar system using MWNTs as reinforcement because of the higher aspect ratio of the RGO laminates with respect to the MWNTs. Finally, a preliminary mechanism to explain the influence of the surface chemistry of the graphitic laminates is proposed. This last point will be analyzed in more detail in a future work.

ASSOCIATED CONTENT

Supporting Information. FTIR spectra of composites of GO and PVC before and after reduction with $NaBH_4$, SEM images of nanocomposites prepared by the two procedures, TGA curves of all samples, and variation of T_g of samples esterified with CNTs and GO with the degree of modification. This material is available free of charge via the Internet at http://pubs.acs.org.

AUTHOR INFORMATION

Corresponding Author
*Telephone: +34-915622900 x208. Fax: +34-915644853. E-mail: horacio@ictp.csic.es.

ACKNOWLEDGMENT

Financial support from the Spanish Ministry of Science and Innovation, MICINN (MAT2009-09335), is gratefully acknowledged. H.J.S. wishes to thank MICINN for a Ramón y Cajal Senior Research Fellowship. The authors thank Dr. Gary Ellis for helpful discussions.

REFERENCES

(1) Geim, A. K.; Novoselov, K. S. *Nat. Mater.* **2007**, *6*, 183–191.
(2) Salavagione, H. J.; Martínez, G.; Ellis, G. *Physics and Applications of Graphene: Experiments*; INTECH: Rijeka, Croatia, 2011; in press, ISBN: 978-953-307-350-7
(3) Ramanathan, T.; Abdala, A. A.; Stankovich, S.; Dikin, D. A.; Herrera-Alonso, M.; Piner, R. D.; Adamson, D. H.; Schniepp, H. C.; Chen, X.; R. S. Ruoff, R. S.; Nguyen, S. T.; Aksay, I. A.; Prud'Homme, R. K.; Brinson, L. C. *Nat. Nanotech.* **2008**, *3*, 327–331.
(4) Stankovich, S.; Dikin, D. A.; Dommett, G. H. B.; Kohlhaas, K. M.; Zimney, E. J.; Stach, E. A.; Piner, R. D.; Nguyen, S. T.; Ruoff, R. S. *Nature* **2006**, *442*, 282–286.
(5) Vickery, J. L.; Patil, A. J.; Mann, S. *Adv. Mater.* **2009**, *21*, 2180–2184.
(6) Yang, H.; Shan, C.; Li, F.; Zhang, Q.; Han, D.; Niu, L. *J. Mater. Chem.* **2009**, *19*, 8856–8860.
(7) Villar-Rodil, S.; Paredes, J. I.; Martínez-Alonso, A.; Tascón, J. M. D. *J. Mater. Chem.* **2009**, *19*, 3591–3593.
(8) Salavagione, H. J.; Martínez, G.; Gómez, M. A. *J. Mater. Chem.* **2009**, *19*, 5027–5032.
(9) Kim, H.; Miura, Y.; Macosko, C. W. *Chem. Mater.* **2010**, *22*, 3441–3450.
(10) Eda, G.; Chhowalla, M. *Nano Lett.* **2009**, *9*, 814–818.
(11) Bao, Q.; Zhang, H.; Yang, J. X., 1; Wang, S.; Tang, D. Y.; Jose, R.; Ramakrishna, S.; Lim, C. T.; Loh, K. P. *Adv. Funct. Mater.* **2010**, *20*, 782–791.
(12) Sternstein, S. S.; Zhu, A. J. *Macromolecules* **2002**, *35*, 7262–7273.
(13) Vaia, R. A.; Maguire, J. F. *Chem. Mater.* **2007**, *19*, 2736–2751.
(14) Huang, Y.; Qin, Y.; Zhou, Y.; Niu, H.; Yu, Z. Z.; Dong, J. Y. *Chem. Mater.* **2010**, *22*, 4096–4102.
(15) Zhao, L.; Zhao, L.; Xu, Y.; Qiu, T.; Zhi, L.; Shi, G. *Electrochim. Acta* **2009**, *55*, 491–497.
(16) Wang, H.; Hao, Q.; Yang, X.; Lu, L.; Wang, X. *Nanoscale* **2010**, *2*, 2164.
(17) Fang, M.; Wang, K.; Lu, H.; Yang, Y.; Nutt, S. *J. Mater. Chem.* **2010**, *20*, 1982–1992.
(18) Ansari, S.; Giannelis, E. P. *J. Polym. Sci., Polym Phys.* **2009**, *47*, 888–897.
(19) Liang, J.; Huang, Y.; Zhang, L.; Wang, Y.; Ma, Y.; Guo, T.; Chen, Y. *Adv. Funct. Mater.* **2009**, *19*, 2297–2302.
(20) Zhao, X.; Zhang, Q.; Chen, D. *Macromolecules* **2010**, *43*, 2357–2363.
(21) Salavagione, H. J.; Gómez, M. A.; Martínez, G. *Macromolecules* **2009**, *42*, 6331–6334.
(22) Vadukumpully, S.; Paul, J.; Mahanta, N.; Valiyaveettil, S. *Carbon* **2011**, *49*, 198–205.
(23) Metrangolo, P.; Meyer, F.; Pilati, T.; Resnati, G.; Terraneo, G. *Angew. Chem. Int.* **2008**, *47*, 6114–6127.
(24) Salavagione, H. J.; Miras, M. C.; Barbero, C. A. *Macromol. Rapid Commun.* **2006**, *27*, 26–30.
(25) Stankovich, S.; Piner, R. D.; Nguyen, S. T.; Ruoff, R. S. *Carbon* **2006**, *44*, 3342–3347.
(26) Salavagione, H. J.; Martínez, G.; Ballesteros, C. *Macromolecules* **2010**, *43*, 9754–9760.
(27) Hummers., W. S.; Offeman, R. E. *J. Am. Chem. Soc.* **1958**, *80*, 1339.
(28) Shimanouchi, T.; Tasumi, M.; Abe, Y. *Makromol. Chem.* **1965**, *86*, 43.
(29) Martínez, G.; Millán, J. *J. Polym. Sci., Polym. Chem.* **2004**, *42*, 6052–6060.
(30) Martínez, G. *J. Polym. Sci., Polym. Chem.* **2006**, *44*, 2476–2486.
(31) Millán, J.; Martínez, G.; Gómez-Elvira, J. M.; Guarrotxena, N.; Tiemblo, P. *Polymer* **1996**, *37*, 219–230and references cited therein.